Bilevel Optimization for Differentially Private Optimization

Ferdinando Fioretto[1] , **Terrence WK Mak**[2] and **Pascal Van Hentenryck**[2]
[1]Syracuse University, [2]Georgia Institute of Technology
ffiorett@syr.edu, wmak@gatech.edu, pvh@isye.gatech.edu

Abstract

This paper studies how to apply differential privacy to constrained optimization problems whose inputs are sensitive. This task raises significant challenges since random perturbations of the input data often render the constrained optimization problem infeasible or change significantly the nature of its optimal solutions. To address this difficulty, this paper proposes a bilevel optimization model that can be used as a post-processing step: It redistributes the noise introduced by a differentially private mechanism optimally while restoring feasibility and near-optimality. The paper shows that, under a natural assumption, this bilevel model can be solved efficiently for real-life large-scale nonlinear nonconvex optimization problems with sensitive customer data. The experimental results demonstrate the accuracy of the privacy-preserving mechanism and showcase significant benefits compared to standard approaches.

1 Introduction

Differential Privacy (DP) [Dwork *et al.*, 2006] is a robust framework used to measure and bound the privacy risks in computations over datasets: It has been successfully applied to numerous applications including histogram queries [Li *et al.*, 2010], census surveys [Abowd, 2018; Fioretto and Van Hentenryck, 2019], linear regression [Chaudhuri *et al.*, 2011] and deep learning [Abadi *et al.*, 2016] to name but a few examples. In general, DP mechanisms ensure privacy by introducing calibrated noise to the outputs or the objective of computations. However, its applications to large-scale, complex constrained optimization problems have been sparse.

This paper considers parametric optimization problems of the form

$$\mathcal{O}(d) = \min_x f(x) \text{ s.t. } g(x,d) \geqslant 0, x \geqslant 0. \qquad \text{(OPT)}$$

where x is a vector of decision variables and d is an input vector. Given a vector d^o of sensitive data, the task is to find a differentially private vector d^* such that $d^* \approx d^o$ and $\mathcal{O}(d^*) \approx \mathcal{O}(d^o)$. Effective solutions to this task are useful in various settings, including the generation of differentially private test cases for (OPT) or in sequential coordination problems, e.g. sequential markets, in which agents need to exchange private versions of their data to solve $\mathcal{O}$. It is possible to use traditional differential privacy techniques (e.g., the ubiquitous Laplace or the Eponential mechanisms) to obtain a private vector $\tilde{d}$ such that $\tilde{d} \approx d^o$. However, in general, the optimization problem (OPT) may not admit any feasible solution for input $\tilde{d}$ or, its objective value $\mathcal{O}(\tilde{d})$ can be far from $\mathcal{O}(d^o)$. See for instance [Mak *et al.*, 2019b] for an illustration of this challenge on Optimal Power Flow (OPF) instances.

This paper aims at remedying this fundamental limitation. Given private versions $\tilde{d}$ of d^o and $\tilde{f}$ of $\mathcal{O}(d^o)$, it proposes a bilevel optimization model that leverages the post-processing immunity of differential privacy to produce a new private vector d^*, based on $\tilde{d}$, such that $\mathcal{O}(d^*) \approx \mathcal{O}(d^o)$. The paper also presents an algorithm that solves the bilevel model optimally under a natural monotonicity assumption. The effectiveness of the approach is demonstrated on large-scale case studies in electrical and gas networks where customer demands are sensitive, including nonlinear nonconvex benchmarks with more than 10^4 variables. The paper generalizes prior approaches designed to release benchmarks in energy systems (e.g., [Mak *et al.*, 2019b]). Its main contributions are as follows:

1. It proposes an algorithm that solves the bilevel optimization model under a natural monotonicity assumption;
2. It demonstrates the effectiveness of the algorithm through case studies: optimal power flow in power network and compressor optimization in gas networks.
3. It empirically validates the monotonicity assumption on these case studies.
4. It demonstrates that optimal solutions to the bilevel model may produce significant improvements in accuracy compared to its relaxations.

2 Preliminaries

The traditional definition of differential privacy [Dwork *et al.*, 2006] aims at protecting the potential participation of an individual in a computation. For optimization problems however, the participants are typically known and the input is a vector $d = \langle d_1, \ldots, d_m \rangle$, where d_i represents a *sensitive quantity* associated with participant i. For instance, d_i may represent the energy consumption of an industrial customer in an elec-

trical transmission system. This privacy notion is best captured by the α-indistinguishability framework proposed by Chatzikokolakis *et al.* [2013] which protects the sensitive data of each individual up to some measurable quantity $\alpha > 0$. As a result, this paper uses an *adjacency relation* $\sim_\alpha$ for input vectors defined as follows:

$$d \sim_\alpha d' \Leftrightarrow \exists i \text{ s.t. } |d_i - {d'}_i| \leqslant \alpha \ \wedge \ d_j = {d'}_j, \forall j \neq i,$$

where d and d' are input vectors to (OPT) and $\alpha > 0$ is a positive real value. This adjacency relation is to protect *an individual value* d_i up to privacy level α even if an attacker acquires information about all other inputs d_j $(j \neq i)$.

Definition 1 (Differential Privacy) *Let $\alpha > 0$. A randomized mechanism $\mathcal{M} : \mathcal{D} \rightarrow \mathcal{R}$ with domain $\mathcal{D}$ and range $\mathcal{R}$ is (ϵ, α)-differential indistinguishable if, for any output response $O \subseteq \mathcal{R}$ and any two* adjacent *input vectors d and d' such that $d \sim_\alpha d'$,*

$$Pr[\mathcal{M}(d) \in O] \leqslant e^\epsilon Pr[\mathcal{M}(d') \in O].$$

Parameter $\epsilon \geqslant 0$ controls the level of *privacy*, with small values denoting strong privacy, while α controls the level of *indistinguishability*. For notational simplicity, this paper assumes that ϵ is fixed to a constant and refers to mechanisms satisfying the definition above as α-indistinguishable.

The post-processing immunity of DP [Dwork and Roth, 2013] guarantees that a private dataset remains private even when subjected to arbitrary subsequent computations.

Theorem 1 (Post-Processing Immunity) *Let $\mathcal{M}$ be an α-indistinguishable mechanism and g be a data-independent mapping from the set of possible output sequences to an arbitrary set. Then, $g \circ \mathcal{M}$ is α-indistinguishable.*

A real function f over a vector d can be made indistinguishable by injecting carefully calibrated noise to its output. The amount of noise to inject depends on the *sensitivity* Δ_f of f defined as $\Delta_f = \max_{d \sim_\alpha d'} \|f(d) - f(d')\|_1$. For instance, querying a customer load from a dataset d corresponds to an identity query whose sensitivity is α. The Laplace mechanism achieves α-indistinguishability by returning the randomized output $f(d) + z$, where z is drawn from the Laplace distribution Lap (Δ_f/ϵ) [Chatzikokolakis *et al.*, 2013].

3 Differentially Private Optimization

3.1 Problem Definition

Consider the parametric optimization problem (OPT), a sensitive vector d^o, an α-indistinguishable version $\tilde{d}$ of d^o, and an approximation $\tilde{f}$ of $\mathcal{O}(d^o)$. For instance, $\tilde{d}$ can be obtained by applying the Laplace mechanism on identity queries on all d_i; $\tilde{f}$ can be a private version of $\mathcal{O}(d^o)$, or the value $\mathcal{O}(d^o)$ itself if it is public (which is typically case when the optimization is a market-clearing mechanism), or an approximation of $\mathcal{O}(d^o)$ obtained using public information only (e.g., a public forecast of d^o). The paper simply assumes that $|\mathcal{O}(d^o) - \tilde{f}| \leqslant \beta^o$ for some value $\beta^o > 0$, which is not restrictive: This assumption obviously holds when f^o is public and it can always be achieved by choosing large enough β^o . The goal is to find a vector d^* using only $\tilde{d}$, $\tilde{f}$, and the definition of (OPT) such that

$$d^* \approx \tilde{d} \text{ and } \mathcal{O}(d^*) \approx \tilde{f}.$$

Observe that, by Theorem 1, d^* will be α-indistinguishable. It will be close to d^o if $\tilde{d}$ is close to d^o. Moreover, (OPT) is feasible for d^* and $\mathcal{O}(d^*)$ will be close to $\mathcal{O}(d^o)$ if $\tilde{f}$ is. The paper uses $\mathcal{S}(d)$ to denote the set of optimal solutions to (OPT), i.e.,

$$\mathcal{S}(d) = \operatorname*{argmin}_x f(x) \text{ s.t. } g(x, d) \geqslant 0, x \geqslant 0,$$

and $\mathcal{F}(d)$ to denote the set of feasible solutions, i.e.,

$$\mathcal{F}(d) = \{x \mid g(x, d) \geqslant 0, x \geqslant 0\}.$$

The paper assumes that $\mathcal{F}(d^o)$ is not empty.

3.2 The Bilevel Optimization Model

The problem defined in Section 3.1 can be tackled by a bilevel optimization model (BL), i.e.,

$$d^* = \operatorname*{argmin}_d \ \|d - \tilde{d}\|_2^2 \qquad \text{(BL1)}$$

$$\text{s.t. } |\mathcal{O}(d) - \tilde{f}| \leqslant \beta. \qquad \text{(BL2)}$$

Its output is a private d^* whose L^2-distance to $\tilde{d}$ is minimized and whose value $\mathcal{O}(d^*)$ is in the interval $[\tilde{f} - \beta, \tilde{f} + \beta]$ for a parameter $\beta \geqslant \beta^o$. To make the bilevel nature more explicit, the above can be reformulated as

$$\min_{d, x^*} \ \|d - \tilde{d}\|_2^2 \qquad \text{(BL1')}$$

$$\text{s.t. } |f(x^*) - \tilde{f}| \leqslant \beta \qquad \text{(BL2')}$$

$$x^* = \operatorname*{argmin}_{x \geqslant 0} f(x) \text{ s.t. } g(x, d) \geqslant 0. \qquad \text{(Follower)}$$

Note that d^o is a feasible solution to (BL), but not necessarily optimal. The set of optimal solutions to (BL) is denoted by $\mathcal{S}^{BL}$ and the set of feasible solutions by $\mathcal{F}^{BL}$.

Theorem 2 *$d^* \in \mathcal{S}^{BL}$ implies $\|d^* - d^o\|_2 \leqslant 2\|\tilde{d} - d^o\|_2$.*

Theorem 2 generalizes a prior result from [Fioretto and Van Hentenryck, 2018]. It implies that, when a Laplace mechanism produces $\tilde{d}$, a solution $d^* \in \mathcal{S}^{BL}$ is no more than a factor of 2 away from optimality since the Laplace mechanism is optimal for identity queries [Koufogiannis *et al.*, 2015]. In other words, (BL) *restores feasibility and near-optimality at a constant cost in accuracy*. In practice, as shown in Section 5, d^* is typically closer to d^o than $\tilde{d}$ is.

Bilevel optimization is computationally challenging. It is strongly NP-hard [Hansen *et al.*, 1992] and even determining the optimality of a solution [Vicente *et al.*, 1994] is NP-hard. The High Point Relaxation (HPR), defined as

$$d^h = \operatorname*{argmin}_{d, x \geqslant 0} \ \|d - \tilde{d}\|_2^2 \qquad \text{(HPR1)}$$

$$\text{s.t. } g(x, d) \geqslant 0 \qquad \text{(HPR2)}$$

$$|f(x) - \tilde{f}| \leqslant \beta \qquad \text{(HPR3)}$$

is an important tool in bilevel optimization and $\mathcal{O}(d^h) \leqslant \mathcal{O}(d^*)$. Theorem 2 also holds for (HPR), i.e., $\|d^h - d^o\|_2 \leqslant 2\|\tilde{d} - d^o\|_2$. The set of optimal solutions to (HPR) is denoted by $\mathcal{S}^{HPR}$ and its set of feasible solutions by $\mathcal{F}^{HPR}$. For simplicity, $(d, x) \in \mathcal{S}^P$ and $d \in \mathcal{S}^P$ are both used to denote an optimal solution to a problem (P) and its projection to d.

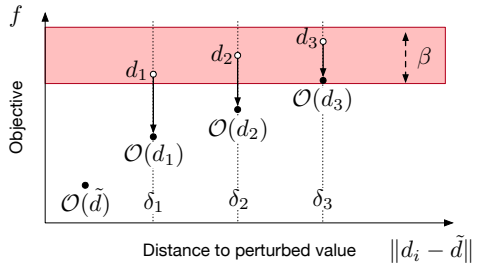

Figure 1: Illustrating the Intuition Underlying $\mathcal{O}^{\uparrow}$.

3.3 Solving the Bilevel Model

While bilevel optimization is, in general, computationally challenging, Model (BL) presents a substantial structure: (Follower) minimizes f but (BL2) restrains it to be in a tight interval and (BL1) keeps the potential solution close to $\tilde{d}$. The proposed solution technique leverages these observations and an additional insight derived from practical applications.

Intuition Consider a pair $(\bar{d}, \bar{x})$ such that $\bar{x} \geqslant 0$, $g(\bar{x}, \bar{d}) \geqslant 0$), and $|f(\bar{x}) - \tilde{f}| \leqslant \beta$. Note that $\bar{x}$ is not necessarily a solution (i.e., a minimizer) to Problem (Follower). However, if the optimal objective value $\mathcal{O}(\bar{d})$ is such that $\mathcal{O}(\bar{d}) \geqslant \tilde{f} - \beta$, then $\bar{d} \in \mathcal{F}^{BL}$. The interesting case is when $\mathcal{O}(\bar{d}) < \tilde{f} - \beta$. The proposed solution method recognizes that, in many optimization problems with sensitive data, $\bar{d}_i$ represents some data about participant i, such as her electricity consumption. Assume, for instance, that $\bar{d}$ represents the customer demands (the reasoning is similar if the data represents prices and reversed if the data represents production capabilities). By increasing $\bar{d}_i$, the value $\mathcal{O}(\bar{d})$ is expected to rise as well. The solution technique exploits this insight: It tries to find solutions that maximize the customer demands while staying within a small distance of $\tilde{d}$. In so doing, it restricts attention to input vectors in the set $\mathcal{N}$ defined as

$$\mathcal{N} = \{d \mid \exists x \geqslant 0 : g(x, d) \geqslant 0 \text{ and } |f(x) - \tilde{f}\| \leqslant \beta\}.$$

Solution Method This section presents an effective algorithm for solving the bilevel optimization problem (BL) when (OPT) is monotone with respect to the sensitive data, capturing the above intuition.

Definition 2 (Monotonicity) (OPT) *is monotone if there exists a function* $m : \Re^m \to \Re$ *such that if, for all* $d^1, d^2 \in \mathcal{N}$, $m(d^1) \geqslant m(d^2) \Rightarrow \mathcal{O}(d^1) \geqslant \mathcal{O}(d^2)$.

Note that the monotonicity assumption applies only to input vectors in $\mathcal{N}$. Computational results will show that this monotonicity property holds on real and realistic benchmarks in energy systems. To solve bilevel optimization problems over a monotone follower, the approach relies on solving optimization problems of the form

$$\begin{aligned} \mathcal{O}^{\uparrow}(\delta) = \max_{d,x \geqslant 0} \quad & m(d) && \text{(PP1)} \\ \text{subject to} \quad & g(x, d) \geqslant 0 && \text{(PP2)} \\ & |f(x) - \tilde{f}| \leqslant \beta && \text{(PP3)} \\ & \|d - \tilde{d}\|_2^2 \leqslant \delta && \text{(PP4)} \end{aligned}$$

Algorithm 1: Solving the BLM Optimization Problem.

Inputs : $\langle \delta^l, \delta^u, \eta \rangle$
Output: An η-approximation to (BL)
1 **while** $\delta^u - \delta^l > \eta$ **do**
2 $\quad \delta \leftarrow \frac{\delta^l + \delta^u}{2}$
3 $\quad$ solve $\mathcal{O}^{\uparrow}(\delta)$ and let $(d^{\uparrow}, x^{\uparrow})$ be an optimal solution
4 $\quad \delta^{\uparrow} \leftarrow \|d^{\uparrow} - \tilde{d}\|$
5 $\quad$ **if** $\mathcal{O}(d^{\uparrow}) > \tilde{f} - \beta$ **then** $\delta^u \leftarrow \delta^{\uparrow}$ **else** $\delta^l \leftarrow \delta$;
6 **return** $\mathcal{S}^{\uparrow}(\delta^u)$

The set of optimal and feasible solutions to $\mathcal{O}^{\uparrow}(\delta)$ are denoted by $\mathcal{S}^{\uparrow}(\delta)$ and $\mathcal{F}^{\uparrow}(\delta)$ respectively. For a given δ, $\mathcal{O}^{\uparrow}(\delta)$ finds a vector $\bar{d} \in \mathcal{N}$ that maximizes $m(\cdot)$ but remains within a distance δ of $\tilde{d}$. Since, by monotonicity, $m(\cdot)$ is a proxy for maximizing $\mathcal{O}(\cdot)$, the optimization can be viewed as searching for a feasible solution of (BL) within a distance δ of $\tilde{d}$ which maximizes $\mathcal{O}(\cdot)$. Figure 1 illustrates the role of $\mathcal{O}^{\uparrow}$. Vector $d_i \in \mathcal{N}$ is the optimal solution of $\mathcal{O}^{\uparrow}(\delta_i)$. As the distance δ_i increases, $d_i = \mathcal{O}^{\uparrow}(\delta_i)$ and $\mathcal{O}(d_i)$ increase as well.

Under the monotonicity assumption, (BL) will be shown equivalent to the following optimization problem:

$$\min_{d, \delta \geqslant 0} \delta \text{ s.t. } d \in S^{\uparrow}(\delta) \ \wedge \ \mathcal{O}(d) \geqslant \tilde{f} - \beta \qquad \text{(BLM)}$$

which is defined only in terms of $\mathcal{O}$ and $\mathcal{O}^{\uparrow}$. Observe that δ is a scalar and hence it is natural to solve (BLM) using binary search as depicted in Algorithm (1). The algorithm receives as input a tuple $\langle \delta^l, \delta^u, \eta \rangle$, where δ^l and δ^u are lower and upper bounds on the optimal value δ^* for (BLM), and produces an η-approximation to (BLM). Algorithm (1) is a simple binary search on the value δ alternating the optimizations of $\mathcal{O}$ and $\mathcal{O}^{\uparrow}$. For a given δ, line 3 solves $\mathcal{O}^{\uparrow}$. If the resulting optimization satisfies the second constraint of (BLM), a new feasible solution to (BL) is obtained and the upper bound can be updated. Otherwise, Algorithm (1) has identified a new lower bound. Note that, in practice, good lower and upper bounds are often available. For instance, it is possible to use an optimal solution d^h of (HPR) and set $\delta^l = \delta^h = \|d^h - \tilde{d}\|_2^2$. To obtain δ^u, one can start with δ^h and continue by doubling its value iteratively until Lemma 1 below applies.

Correctness It remains to prove the correctness of the solution technique. The following two lemmas capture important properties of $\mathcal{O}^{\uparrow}$. The first lemma shows that, when δ is large enough, $\mathcal{O}^{\uparrow}(\delta)$ always returns a feasible solution to (BL).

Lemma 1 *Let* $\delta^o = \|d^o - \tilde{d}\|_2^2 \leqslant \delta^o$ *and* $(d^{\uparrow}, x^{\uparrow}) \in \mathcal{S}^{\uparrow}(\delta^o)$. *Then* $d^{\uparrow} \in \mathcal{F}^{BL}$.

Proof. By definition of δ^o, $d^o \in \mathcal{F}^{\uparrow}(\delta^o)$ and there exists x^o such that the pair (d^o, x^o) satisfies conditions (PP2)–(PP4). Since $(d^{\uparrow}, x^{\uparrow}) \in \mathcal{S}^{\uparrow}(\delta^o)$, $m(d^{\uparrow}) \geqslant m(d^o)$ and, by monotonicity, $\mathcal{O}(d^{\uparrow}) \geqslant \mathcal{O}(d^o) \geqslant \tilde{f} - \beta$. By (PP3), $f(x^{\uparrow}) \leqslant f^o + \beta$ and, by (PP2), $\mathcal{O}(d^{\uparrow}) \leqslant f(x^{\uparrow})$. Hence

$$\tilde{f} + \beta \geqslant f(x^{\uparrow}) \geqslant \mathcal{O}(d^{\uparrow}) \geqslant \mathcal{O}(d^o) \geqslant \tilde{f} - \beta$$

and $d^{\uparrow}$ satisfies (BL2). □

Model 1 $\mathcal{O}_{\text{OPF}}$: AC Optimal Power Flow

variables: $S_i^g, V_i \;\; \forall i \in N, \;\; S_{ij} \;\; \forall (i,j) \in E \cup E^R$

minimize: $\mathcal{O}(\boldsymbol{S^d}) = \sum_{i \in N} c_{2i}(\Re(S_i^g))^2 + c_{1i}\Re(S_i^g) + c_{0i}$ (3)

subject to: $\angle V_i = 0, \;\; i \in N$ (4)

$v_i^l \leqslant |V_i| \leqslant v_i^u \;\; \forall i \in N$ (5)

$\theta_{ij}^l \leqslant \angle(V_i V_j^*) \leqslant \theta_{ij}^u \;\; \forall (i,j) \in E$ (6)

$S_i^{gl} \leqslant S_i^g \leqslant S_i^{gu} \;\; \forall i \in N$ (7)

$|S_{ij}| \leqslant s_{ij}^u \;\; \forall (i,j) \in E \cup E^R$ (8)

$S_i^g - S_i^d = \sum_{(i,j) \in E \cup E^R} S_{ij} \;\; \forall i \in N$ (9)

$S_{ij} = Y_{ij}^* |V_i|^2 - Y_{ij}^* V_i V_j^* \;\; \forall (i,j) \in E \cup E^R$ (10)

Model 2 $\mathcal{O}_{\text{OGF}}$: Optimal Gas Flow

variables: $p_i, q_i \; \forall i \in \mathcal{J}, \; q_{ij} \; \forall (i,j) \in \mathcal{P}, \; R_{ij} \; \forall (i,j) \in \mathcal{C}$

minimize: $\mathcal{O}(\boldsymbol{q}) = \sum_{(i,j) \in C} \mu^{-1} |q_{ij}| (\max\{R_{ij}, 1\}^{2(\gamma-1)/\gamma} - 1)$ (11)

subject to: $\sum_{(i,j) \in \mathcal{P}} q_{ij} - \sum_{(j,i) \in \mathcal{P}} q_{ji} = q_i, \;\; \forall i \in \mathcal{J}$ (12)

${p_i}^l \leqslant p_i \leqslant {p_i}^u \;\; \forall i \in N, \;\; {q_{ij}}^l \leqslant q_{ij} \leqslant {q_{ij}}^u \;\; \forall (i,j) \in \mathcal{P}$ (13)

${R_{ij}}^l \leqslant R_{ij} \leqslant {R_{ij}}^u \;\; \forall (i,j) \in \mathcal{C}$ (14)

$p_i = p_i^T \;\; \forall i \in \mathcal{J}^B, q_i = 0 \;\; \forall i \in \mathcal{J}^T, q_i = q_i^d \;\; i \in \mathcal{J}^D$ (15)

$R_{ij}^2 p_i^2 - p_j^2 = L_{ij} \frac{\lambda a^2}{D_{ij} A_{ij}^2} q_{ij} |q_{ij}| \;\; \forall (i,j) \in \mathcal{C}$ (16)

$p_i^2 - p_j^2 = L_{ij} \frac{\lambda a^2}{D_{ij} A_{ij}^2} q_{ij} |q_{ij}| \;\; \forall (i,j) \in \mathcal{P} - \mathcal{C}$ (17)

The second lemma shows that there is no feasible solution to (BL) within distance $\dot{\delta}$ of $\tilde{d}$ when $\mathcal{O}(\dot{\delta})$ returns a solution d that violates (BL2).

Lemma 2 *Let $(\dot{d}, \dot{x}) \in \mathcal{S}^{\uparrow}(\dot{\delta})$ and $\mathcal{O}(\dot{d}) < \tilde{f} - \beta$. Then,*

$$\forall d^f \in \mathcal{F}^{BL} : \|d^f - \tilde{d}\|_2^2 > \dot{\delta}.$$

Proof. Consider $d^f \in \mathcal{F}^{BL}$ and assume that $\|d^f - \tilde{d}\|_2^2 \leqslant \dot{\delta}$, which implies that $d^f \in \mathcal{F}^{\uparrow}(\dot{\delta})$. By optimality of $\dot{d}$, $m(\dot{d}) \geqslant m(d^f)$ and, by monotonicity, $\mathcal{O}(\dot{d}) \geqslant \mathcal{O}(d^f)$. By (BL2), $\mathcal{O}(d^f) \geqslant \tilde{f} - \beta$ which contradicts $\mathcal{O}(\dot{d}) < \tilde{f} - \beta$. □

These two lemmas make it possible to prove the equivalence of (BL) and (BLM) when (OPT) is monotone.

Theorem 3 *When (OPT) is monotone,* (BL) *and* (BLM) *are equivalent.*

Proof. Let (d^*, δ^*) be the optimal solution to (BLM). Such a solution always exists by Lemma 1 and $\|d^* - \tilde{d}\|_2^2 \leqslant \delta^*$. By definition of $\mathcal{O}^{\uparrow}$, $\mathcal{F}(d^*) \neq \varnothing$ and $\mathcal{O}(d^*) \leqslant \tilde{f} + \beta$. Since $\mathcal{O}(d^*) \geqslant \tilde{f} - \beta$ by definition of (BLM), $d^* \in \mathcal{F}^{BL}$.

Consider now $\delta^- < \delta^*$ and a solution $d^- \in \mathcal{S}^{\uparrow}(\delta^-)$. If such a solution exists, $\mathcal{O}(d^-) < f^o - \beta$ by optimality of δ^*. By Lemma 2, it comes that $\forall d^f \in \mathcal{F}^{BL} : \|d^f - \tilde{d}\|_2^2 > \delta^-$. Hence, d^* is also optimal for (BL). □

It remains to show that the algorithm computes an η-approximation.

Theorem 4 *Algorithm* (1) *computes an η-approximation of* (BL) *when* (OPT) *is monotone.*

Proof. Let d^* be an optimal solution to (BL). Upon termination of Algorithm (1), it comes that $\delta^l \leqslant \|d^* - \tilde{d}\|_2^2 \leqslant \delta^u$. Moreover, if $d^u \in S^{\uparrow}(\delta^u)$, it follows that $\|d^u - \tilde{d}\|_2^2 \leqslant \delta^u$. Hence, $\delta^l \leqslant \|d^* - \tilde{d}\|_2^2 \leqslant \|d^u - \tilde{d}\|_2^2 \leqslant \delta^u$. □

4 Applications on Energy Systems

This section describes two substantial case studies for evaluating the privacy mechanism: optimal power flow in electricity networks and optimal compressor optimization in gas networks. Both models are nonlinear and nonconvex.

Optimal Power Flow *Optimal Power Flow (OPF)* is the problem of finding the best generator dispatch to meet the demands in a power network. A power network $\boldsymbol{\mathcal{N}}$ can be represented as a graph (N, E), where the nodes in N represent buses and the edges in E represent lines. The edges in E are directed and E^R is used to denote those arcs in E but in reverse direction. The AC power flow equations are based on complex quantities for current I, voltage V, admittance Y, and power S, and these equations are a core building block in many power system applications. Model 1 shows the AC OPF formulation, with variables/quantities shown in the complex domain. Superscripts u and l are used to indicate upper and lower bounds for variables. The objective function $\mathcal{O}(\boldsymbol{S^g})$ captures the cost of the generator dispatch, with $\boldsymbol{S^g}$ denoting the vector of generator dispatch values $(S_i^g \mid i \in N)$. Constraint (4) sets the reference angle to zero for the slack bus $i \in N$ to eliminate numerical symmetries. Constraints (5) and (6) capture the voltage and phase angle difference bounds. Constraints (7) and (8) enforce the generator output and line flow limits. Finally, Constraints (9) capture Kirchhoff's Current Law and Constraints (10) capture Ohm's Law.

Optimal Compressor Optimization *Optimal Gas Flow (OGF)* is the problem of finding the best compression control to maintain pressure requirements in a natural gas pipeline system. A natural gas network can be represented as a directed graph $\boldsymbol{\mathcal{N}} = (\mathcal{J}, \mathcal{P})$, where a node $i \in \mathcal{J}$ represents a junction point and an arc represents a pipeline $(i,j) \in \mathcal{P}$ represent the edges. Compressors ($\mathcal{C} \subseteq \mathcal{P}$) are installed in a subset of the pipelines for boosting the gas pressure p in order to maintain pressure requirements for gas flow q. The set $\mathcal{J}^D$ of gas demands and the set $\mathcal{J}^T$ of transporting nodes are modeled as junction points, with net gas flow q_i set to the gas demand (q_i^d) and zero respectively. For simplicity, the paper assumes no pressure regulation and losses within junction nodes and gas flow/flux are conserved throughout the system. A subset $\mathcal{J}^B \in \mathcal{J}$ of the nodes are regulated with constant pressure p_i^T. The length of pipe (i,j) is denoted by L_{ij}, its diameter by D_{ij}, and its cross-sectional area by A_{ij}. Universal quantities include isentropic coefficient γ, compressor efficiency factor μ, sound speed a, and gas friction factor λ. Model 2 depicts the OGF formulation. The objective function $\mathcal{O}(\boldsymbol{q})$ captures the compressor costs using the compressor control values $(R_{ij} \mid (i,j) \in \mathcal{C})$. Constraints (12) capture the

flow conversation equations. Constraints (13) and (14) capture the pressure, flux flow, and compressor control bounds. Constraints (15) set the boundary conditions for the demands and the regulated pressures. Finally, Constraints (16) and (17) capture the steady-state isothermal gas flow equation.

Obfuscation In both networks, customer demands are sensitive and are associated with customer activities. These quantities always appear in the flow conservation constraints, which are linear. Increasing these values obviously requires more (electricity and gas) production and hence one can expect the cost to increase. This is not always the case, because of the engineering constraints on voltages and pressures and the lower bounds of the production units, for instance. However, in practice, because of reliability constraints, these constraints are rarely binding at optimality and one may expect the systems to behave monotonically around the optimality point. The above is validated in the experimental results.

5 Experimental Evaluation

Setting The experiments were performed on a variety of NESTA power systems [Coffrin *et al.*, 2014] and natural gas test systems from [Mak *et al.*, 2019a], including test instances from GasLib [Pfetsch *et al.*, 2015]. Parameter ϵ is fixed to 1.0 and the *indistinguishability level* α varies from 10^{-1} to 10^{1} (in per unit notation). The *fidelity* parameter β varies from 0.1% to 10% of value $\tilde{f} = f^o$. Convergence parameter η is set to 10^{-3} (in per unit). The lower bounds and upper bounds are initialized as specified in prior sections. The solution technique is limited to 3000 calls to $\mathcal{O}^\uparrow$. The models are implemented with PowerModels.jl [Coffrin *et al.*, 2018] with the nonlinear solver IPOPT [Wächter and Biegler, 2006]. Note that some of the test cases have more than 10^4 variables.

Behavior of the Solution Technique Figure 2 shows how the costs ($\mathcal{O}$ and $\mathcal{O}^\uparrow$) and L^2-Distance to $\tilde{\delta}$ typically change when running Algorithm 1 and its initialization. The L^2-Distance to $\tilde{d}$ increases initially to find a solution within the feasible cost range (shaded area). The binary search then finds the optimal distance in a few iterations. (PP4) is usually binding when optimizing $\mathcal{O}^\uparrow$.

Convergence and Computational Efficiency The experimental results demonstrate the robustness and scalability of the approach. Tables 1 and 2 depict the average CPU times (in seconds) and average number of calls to $\mathcal{O}^\uparrow$ (and thus $\mathcal{O}$) also over 50 runs. All instances (except one[1]) converge with a very small number of iterations. Even large-scale test cases with more than 10^4 variables are solved in a few iterations. *The bilevel model is thus a truly practical approach to demand obfuscation of these networks.*

Monotonicity Figures 3 and 4 illustrate the interpolation of the optimal values $\mathcal{O}^\uparrow$ (y-axis) with the respect to their distances to $\tilde{\delta}$ (x-axis) obtained while solving the bilevel model. The shaded area shows the feasible cost range. The results summarize 50 runs (each with a different random seed), each

[1]The failure to converge on IEEE-73 (marked with a superscript) is due to a poor starting point from the HPR.

α	0.1	1.0	10.0	0.1	1.0	10.0
Benchmark	Time (s)	Time (s)	Time (s)	Opt.	Opt.	Opt.
case14_ieee	0.71	0.58	1.01	10.22	4.40	6.10
case24_ieee_rts	1.52	1.40	2.30	8.90	4.14	5.10
case29_edin	0.67	36.84	23.50	1.00	40.36	27.78
case30_as	0.90	0.90	0.85	4.62	4.28	3.80
case30_fsr	1.28	1.07	0.66	6.24	4.70	2.82
case30_ieee	0.84	1.22	1.33	5.14	5.86	6.06
case39_epri	1.16	6.92	1.29	6.32	21.50	3.14
case57_ieee	1.77	4.22	10.31	4.98	3.72	7.94
case73_ieee_rts	6.20	2.17	11.57[1]	9.88	1.62	66.54
case89_pegase	9.23	13.56	17.60	6.04	5.26	7.82
case118_ieee	10.15	10.71	9.77	10.08	5.96	6.42
case162_ieee_dtc	10.04	35.18	53.72	4.88	9.68	8.82
case189_edin	2.98	53.40	58.08	2.16	7.98	8.18
case240_wecc	12.34	117.78	148.16	1.16	10.88	10.10
case300_ieee	1621.78	360.99	301.32	8.90	7.98	10.32
case1354_pegase	15.90	2172.23	2363.19	1.16	7.68	9.10
case1394sop_eir	70.78	777.66	1427.87	3.72	6.12	5.40
case1397sp_eir	146.47	1298.15	660.12	3.90	6.40	4.60
case1460wp_eir	157.06	1418.58	728.84	4.72	6.90	5.66

Table 1: OPF: Average CPU times and number of optimizations (50 runs) for parameters $\alpha = \{0.1, 1.0, 10.0\}$ and $\beta = 1\%$.

α	0.1	1.0	2.0	0.1	1.0	2.0
Benchmark	Time (s)	Time (s)	Time (s)	Opt.	Opt.	Opt.
24-pipe	2.34	0.67	1.77	20.56	6.20	6.22
GasLib-40	34.74	141.16	132.65	26.50	33.48	28.82
GasLib-135	21.63	28.91	214.57	12.96	8.74	25.80

Table 2: OGF: Average CPU times and number of optimizations (50 runs) for parameters $\alpha = \{0.1, 1.0, 2.0\}$ and $\beta = 1\%$.

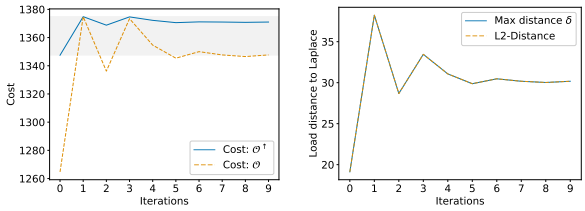

Figure 2: Gaslib-135: OGF costs and L^2-distance to $\tilde{\delta}$ as a function of the number of iterations for parameters $\alpha = 0.1$ and $\beta = 1\%$.

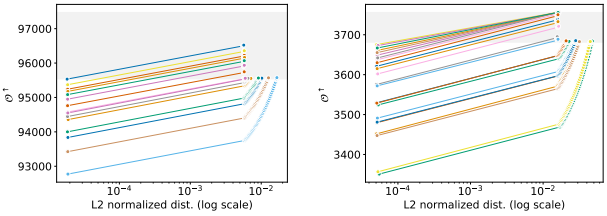

Figure 3: IEEE-39 (left) IEEE-118 (right): OPF cost as a function of the L^2-distance to $\tilde{\delta}$ for parameters $\alpha = 0.1$ and $\beta = 1\%$.

represented by a colored curve. *As can be seen, the monotonicity property holds in these real networks.* Note also the single points in the gas plot: These are cases where the high-point relaxation can be made optimal in one iteration.

The Benefits of the Bilevel Model Tables 3 and 4 show the benefits of the bilevel model compared to the HPR. The HPR returns a solution d^h in $\mathcal{N}$ with the smallest distance

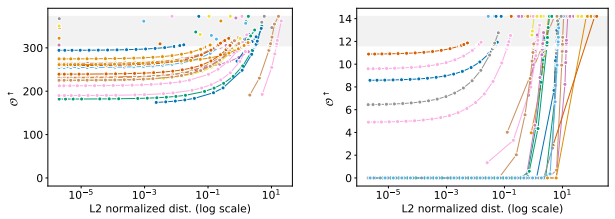

Figure 4: 24-pipe (left) Gaslib-40 (right): OGF cost as a function of the L^2-distance to $\tilde{\delta}$ for parameters $\alpha = 0.1$ and $\beta = 10\%$.

	Bi-level			High-point		
$\beta(\%)$	10%	1%	0.1%	10%	1%	0.1%
case14_ieee	0.1	0.1	0.0	-4.9	-6.2	-6.3
case24_ieee_rts	0.0	0.4	0.1	-0.1	-1.6	-1.9
case29_edin	-0.0	-0.0	0.0	-0.0	-0.0	-0.1
case30_as	0.7	0.3	-0.1	-1.1	-2.3	-2.4
case30_fsr	-0.1	0.3	-0.1	-6.2	-6.8	-6.9
case30_ieee	-0.3	0.1	0.0	-2.7	-1.8	-1.6
case39_epri	-0.2	-0.0	0.0	-0.2	-0.4	-0.7
case57_ieee	1.5	0.4	0.1	1.4	-0.6	-1.0
case73_ieee_rts	-0.4	0.1	0.0	-0.4	-1.1	-1.4
case89_pegase	-0.3	-0.1	0.0	-0.3	-0.4	-0.6
case118_ieee	-0.0	0.3	0.0	-0.0	-1.6	-2.0
case162_ieee_dtc	2.6	0.5	0.1	2.3	-0.1	-0.7
case189_edin	9.2	1.0	0.1	9.2	0.8	-0.1
case240_wecc	0.4	0.1	0.0	0.4	0.1	-0.2
case300_ieee	8.9	0.9	0.1	8.8	0.9	0.1
case1354_pegase	0.0	0.0	0.0	0.0	0.0	-0.1
case1394sop_eir	9.8	1.0	0.1	10.3	1.2	0.3
case1397sp_eir	10.0	1.0	0.1	10.5	2.0	0.7
case1460wp_eir	9.8	1.0	0.1	14.6	1.5	0.7

Table 3: OPF test cases: Average OPF cost difference (in %) for parameters $\alpha = 0.1$ and $\beta = \{10\%, 1\%, 0.1\%\}$.

	Bi-level			High-point		
$\beta(\%)$	10%	1%	0.1%	10%	1%	0.1%
24-pipe	-3.1	-0.3	0.0	-12.1	-13.7	-14.1
gaslib-40	2.5	0.3	0.0	-31.5	-38.1	-39.0
gaslib-135	1.3	0.2	0.0	-37.3	-38.4	-41.6

Table 4: OGF test cases: Average OGF cost differences (in %) for parameters $\alpha = 0.1$ and $\beta = \{10\%, 1\%, 0.1\%\}$.

to $\tilde{d}$. However, it is typically the case that $\mathcal{O}(d^h) < \tilde{f} - \beta$. The tables report the relative distance of $\mathcal{O}(d^*)$ and $\mathcal{O}(d^h)$ to f^0 for various values of β. Table 4 shows that, on the gas networks, the bilevel model produces several orders of magnitude improvements over the HPR. The gains are less pronounced on the electricity systems, but remain substantial. *Notice that a few percents in the energy sector correspond to hundreds of millions of dollars*.

Obfuscation Quality Tables 5 and 6 report the L^2-distances to the original loads for the high-point relaxation, the bilevel model, and the load vector $\tilde{d}$ (which typically produces infeasible problems). The results are averaged over 50 runs. The results show that the fidelity of the bilevel model (i.e., how close d^* is to d^o) is extremely high, and often improves over the fidelity of the HPR. Finally, the bilevel model has a much higher fidelity than the Laplace mechanism.

	Bi-level			High-point			Laplace		
α (p.u.)	0.1	1.0	10.0	0.1	1.0	10.0	0.1	1.0	10.0
case14_ieee	0.67	4.48	10.32	0.67	4.51	10.60	0.71	7.08	70.82
case24_ieee_rts	0.13	1.11	3.61	0.13	1.11	3.63	0.13	1.34	13.39
case29_edin	0.01	0.09	0.82	0.01	0.09	0.82	0.01	0.09	0.87
case30_as	0.84	3.34	4.45	0.84	3.35	4.49	0.97	9.74	97.43
case30_fsr	1.42	5.47	7.40	1.43	5.49	7.47	1.66	16.61	166.14
case30_ieee	0.88	3.86	5.46	0.88	3.88	5.60	0.97	9.74	97.43
case39_epri	0.06	0.60	2.44	0.06	0.60	2.44	0.06	0.62	6.24
case57_ieee	0.34	2.38	6.64	0.34	2.42	7.56	0.35	3.51	35.14
case73_ieee_rts	0.13	1.11	3.65	0.13	1.11	3.67	0.13	1.32	13.19
case89_pegase	0.06	0.53	2.64	0.06	0.53	2.86	0.06	0.56	5.60
case118_ieee	0.40	3.03	6.85	0.40	3.04	6.87	0.40	3.99	39.89
case162_ieee_dtc	0.09	0.68	1.59	0.10	0.69	1.61	0.10	0.96	9.62
case189_edin	0.34	2.05	3.92	0.34	2.07	4.18	0.35	3.50	35.05
case240_wecc	0.01	0.12	0.99	0.01	0.12	1.01	0.01	0.12	1.23
case300_ieee	0.10	0.85	3.69	0.10	0.86	4.46	0.11	1.07	10.65
case1354_pegase	0.14	1.26	5.47	0.14	1.26	6.21	0.14	1.36	13.59

Table 5: OPF test cases: Average distance (L2, normalized to original scale) between obfuscated and original solutions for parameters $\alpha = \{0.1, 1.0, 10.0\}$ and $\beta = 1\%$.

	Bi-level			High-point			Laplace		
α (p.u.)	0.1	0.4	1.0	0.1	0.4	1.0	0.1	0.4	1.0
24-pipe	0.32	1.24	2.68	0.34	1.29	2.71	0.36	1.43	3.58
gaslib-40	2.04	7.66	22.13	1.95	7.51	16.54	2.01	8.03	20.07
gaslib-135	0.72	2.78	7.30	0.72	2.75	6.46	0.72	2.88	7.19

Table 6: OGF test cases: Average distance (L2, normalized to original scale) between obfuscated and original solutions for parameters $\alpha = \{0.1, 0.4, 1.0\}$ and $\beta = 1\%$.

6 Related Work

This paper generalizes the results from [Mak *et al.*, 2019b] on power systems to a broader context: It presents them in a general setting, formalizes the monotonicity property, and proves the optimality of the algorithm under the monotonicity assumption. It also presents novel experimental results on gas networks and empirical evidence for the monotonicity assumption. The HPR was proposed as a post-processing step for power systems in [Fioretto *et al.*, 2018]. Zhou *et al.* [2019] presents a particularly interesting relaxed notion of a (stronger) monotonicity property for a DC-OPF operator and shows how to use it to compute the operator sensitivity. Finally, Karapetyan *et al.* [2017] quantifies empirically the trade-off between privacy and utility in demand response systems: They analyzed the effects of the Laplace mechanism.

7 Conclusion

This paper presented a bilevel optimization model for post-processing the differentially private input of a constrained optimization problem. The model restores the feasibility and near-optimality of the optimization problem. The paper shows that the bilevel model can be solved effectively under a natural monotonicity assumption by alternating the solving of the follower problem and the solving of a novel optimization model that maximizing a proxy of the true objective. Experimental results on large-scale nonconvex constrained optimization problems with more than 10^4 variables demonstrate the accuracy, efficiency, and benefits of the approach. They also validate the monotonicity assumptions empirically. Future work will be devoted to understanding and characterizing theoretically the solution space around optimal solutions.

References

[Abadi *et al.*, 2016] Martin Abadi, Andy Chu, Ian Goodfellow, H Brendan McMahan, Ilya Mironov, Kunal Talwar, and Li Zhang. Deep learning with differential privacy. In *Proceedings of the 2016 ACM SIGSAC Conference on Computer and Communications Security*, pages 308–318. ACM, 2016.

[Abowd, 2018] John M Abowd. The us census bureau adopts differential privacy. In *Proceedings of the 24th ACM SIGKDD International Conference on Knowledge Discovery & Data Mining*, pages 2867–2867. ACM, 2018.

[Chatzikokolakis *et al.*, 2013] Konstantinos Chatzikokolakis, Miguel E Andrés, Nicolás Emilio Bordenabe, and Catuscia Palamidessi. Broadening the scope of differential privacy using metrics. In *International Symposium on Privacy Enhancing Technologies Symposium*, pages 82–102. Springer, 2013.

[Chaudhuri *et al.*, 2011] Kamalika Chaudhuri, Claire Monteleoni, and Anand D Sarwate. Differentially private empirical risk minimization. *Journal of Machine Learning Research*, 12(Mar):1069–1109, 2011.

[Coffrin *et al.*, 2014] Carleton Coffrin, Dan Gordon, and Paul Scott. Nesta, the NICTA energy system test case archive. *CoRR*, abs/1411.0359, 2014.

[Coffrin *et al.*, 2018] Carleton Coffrin, Russell Bent, Kaarthik Sundar, Yeesian Ng, and Miles Lubin. Powermodels.jl: An open-source framework for exploring power flow formulations. In *PSCC*, pages 1–8, June 2018.

[Dwork and Roth, 2013] Cynthia Dwork and Aaron Roth. The algorithmic foundations of differential privacy. *Theoretical Computer Science*, 9(3-4):211–407, 2013.

[Dwork *et al.*, 2006] Cynthia Dwork, Frank McSherry, Kobbi Nissim, and Adam Smith. Calibrating noise to sensitivity in private data analysis. In *TCC*, volume 3876, pages 265–284. Springer, 2006.

[Fioretto and Van Hentenryck, 2018] Ferdinando Fioretto and Pascal Van Hentenryck. Constrained-based differential privacy: Releasing optimal power flow benchmarks privately. In *Proceedings of Integration of Constraint Programming, Artificial Intelligence, and Operations Research (CPAIOR)*, pages 215–231, 2018.

[Fioretto and Van Hentenryck, 2019] Ferdinando Fioretto and Pascal Van Hentenryck. Differential privacy of hierarchical census data: An optimization approach. In *Principles and Practice of Constraint Programming - 25th International Conference, CP*, pages 639–655, 2019.

[Fioretto *et al.*, 2018] Ferdinando Fioretto, Chansoo Lee, and Pascal Van Hentenryck. Constrained-based differential privacy for private mobility. In *Proceedings of the International Joint Conference on Autonomous Agents and Multiagent Systems (AAMAS)*, 2018.

[Hansen *et al.*, 1992] Pierre Hansen, Brigitte Jaumard, and Gilles Savard. New branch-and-bound rules for linear bilevel programming. *SIAM J. Sci. and Stat. Comput.*, 13(5):1194–1217, 1992.

[Karapetyan *et al.*, 2017] Areg Karapetyan, Syafiq Kamarul Azman, and Zeyar Aung. Assessing the privacy cost in centralized event-based demand response for microgrids. *CoRR*, abs/1703.02382, 2017.

[Koufogiannis *et al.*, 2015] Fragkiskos Koufogiannis, Shuo Han, and George J Pappas. Optimality of the laplace mechanism in differential privacy. *arXiv preprint arXiv:1504.00065*, 2015.

[Li *et al.*, 2010] Chao Li, Michael Hay, Vibhor Rastogi, Gerome Miklau, and Andrew McGregor. Optimizing linear counting queries under differential privacy. In *Proceedings of the twenty-ninth ACM SIGMOD-SIGACT-SIGART symposium on Principles of database systems*, pages 123–134. ACM, 2010.

[Mak *et al.*, 2019a] Terrence W. K. Mak, Pascal Van Hentenryck, Anatoly Zlotnik, and Russell Bent. Dynamic compressor optimization in natural gas pipeline systems. *INFORMS Journal on Computing*, 31(1):40–65, 2019.

[Mak *et al.*, 2019b] Terrence W.K. Mak, Ferdinando Fioretto, Lyndon Shi, and Pascal Van Hentenryck. Privacy-preserving power system obfuscation: A bilevel optimization approach. *IEEE Transactions on Power Systems*, to appear, 2019.

[Pfetsch *et al.*, 2015] M. Pfetsch, A. Fügenschuh, B. Geißler, N. Geißler, R. Gollmer, B. Hiller, J. Humpola, T. Koch, T. Lehmann, A. Martin, A. Morsi, J. Rövekamp, L. Schewe, M Schmidt, R. Schultz, R. Schwarz, J. Schweiger, C. Stangl, M. Steinbach, S. Vigerske, and B. Willert. Validation of nominations in gas network optimization: Models, methods, and solutions. *Optimization Methods and Software*, 30(1):15–53, 2015.

[Vicente *et al.*, 1994] Luis Vicente, Gilles Savard, and Joaquim Júdice. Descent approaches for quadratic bilevel programming. *J. of optimization theory and applications*, 81(2):379–399, 1994.

[Wächter and Biegler, 2006] Andreas Wächter and Lorenz T. Biegler. On the implementation of an interior-point filter line-search algorithm for large-scale nonlinear programming. *Mathematical Programming*, 106(1):25–57, 2006.

[Zhou *et al.*, 2019] Fengyu Zhou, James Anderson, and Steven H Low. Differential privacy of aggregated dc optimal power flow data. *arXiv preprint arXiv:1903.11237*, 2019.